Semiannual Report

Radiometric Calibration of the Earth Observing System's Imaging Sensors

Covering the period of:

May 1987 through November 1987

for

NASA GRANT NAGW-896

Submitted by:

P. N. Slater
Principal Investigator and
Chairman Committee on Remote Sensing
Optical Sciences Center
University of Arizona

December 1987

TABLE OF CONTENTS

I. INTRODUCTION

This is the semiannual report on grant number NAGW-896 entitled "Radiometric Calibration of the Earth Observing System's Imaging Sensors." During this period the following people have contributed to the work described here:

S. F. Biggar	Optical Sciences
R. J. Bartell	Optical Sciences
R. G. Holm	Optical Sciences, now JPL
R. D. Jackson	Agricultural Research Service USDA, Phoenix
M. S. Moran	Agricultural Research Service USDA, Phoenix
R. P. Santer	Optical Sciences, now back at the University of Lille, France
P. N. Slater	Optical Sciences
P. M. Teillet	Optical Sciences, on leave from the Canada Centre for Remote Sensing
B. Yuan	Optical Sciences, on leave from the People's Republic of China

Our work is concerned with developing new redundant methods for the in-flight absolute radiometric calibration of satellite multispectral imaging systems and refining the accuracy of methods already in use. The work is principally directed at the calibration of the MODIS-N and HIRIS systems planned for Eos.

This report is divided into four parts. First is a discussion of calibration philosophy, requirements, and methods written by P. N. Slater as part of a report for an Eos calibration meeting held at JPL on 25 September 1987 at which MODIS-N and HIRIS representatives were present. Second is a preliminary draft of a paper entitled "Surface Reflectance Factor Retrieval from Thematic Mapper Data." Third is a summary report of vicarious methods for calibration of low spatial resolution systems. Fourth is a theoretical introduction to a new vicarious method of calibration using the ratio of diffuse-to-global irradiance at the earth's surfaces as the key input. This may provide an additional independent method for in-flight calibration.

Significant work on the in-flight calibration of AVIRIS and the laboratory calibration of standard reflectance panels has also been conducted during this period. This work will be discussed in detail in our May 1988 report.

II. CALIBRATION OF MULTISPECTRAL SPACE SYSTEMS

The following was written as part of a report on Eos calibration philosophy, requirements and methods for an Eos calibration meeting held at JPL on 25 September 1987 at which MODIS-N and HIRIS representatives were present.

The justifications for the absolute radiometric calibration of space multi-spectral imaging instruments are:

1. The retrieval of surface reflectances or other physical properties using atmospheric correction methods.
2. The determination of the inputs to energy balance relationships.
3. The determination of chlorophyll concentrations.
4. The monitoring of changes in sensor response with time for long-term science studies.

Three critical requirements need to be met to assure the reliability and utility of absolute radiometric calibration.

1. That several independent, precise methods provide the same result within their uncertainty limits, because it is only through redundancy that we can be sure systematic errors and biases in the calibrations have been minimized.

2. That the calibration simulate, to the closest extent possible, the operational image acquisition mode of the instrument. For example, the exclusion of out-of field radiation in the calibration geometry could give rise to a bias of several percent in the calibration, as it ignores a large proportion of the average stray-light level in the instrument. Furthermore, the conventional static, uniform radiance field, macro-image, absolute calibration does not simulate the dynamic, variable radiance field, micro-image response of the system.

3. That the spectral responses of the instruments need to be characterized pre-flight and in-flight. For example, bandpass shifts in spectral filters can be of the order of 10 nm, sufficient to seriously affect data interpretation.

For these reasons several independent calibrations should be conducted in-flight, and cross-calibrations should be conducted between similar instruments both preflight and in-flight. Also, in addition to conventional calibration procedures, detailed investigations should be conducted preflight to characterize the dynamic response of the systems.

For convenience, the following is divided into preflight and in-flight issues.

Preflight

CALIBRATION

Preflight calibration should be conducted with the goal of a 5% uncertainty under thermal vacuum conditions. It is anticipated that an integrating sphere or hemisphere would be used for this purpose. (It is unlikely that the cost related to devising high accuracy preflight procedures is warranted due (1) to the inadequate simulation of operational conditions and (2) to the unknown discontinuities anticipated in the calibration during launch and orbit insertion.)

CHARACTERIZATION

The instruments need to be characterized in terms of:

1. Out-of-field response;
2. Recovery time after saturation (or high signal level) e.g., cloud-to-sea-to-cloud. This is often referred to as the memory effect;
3. Linearity of A/D converter;
4. Detector cross-talk;
5. Polarization-induced signal changes particularly as a function of pointing angle;
6. "Vacuum-thermal shift" effects, e.g., changes in spectral bandpasses of interference filters due to temperature and vacuum conditions.

CROSS-CALIBRATION

Portable standard spectroradiometers and/or radiance sources need to be developed to intercompare accurately the outputs of calibration sources at different facilities. If practical and possible, the same procedures should be followed for characterizing the responses of all instruments.

In-Flight Radiometric Calibration

Being the most important phase of the calibration, in-flight radiometric calibration merits the greatest degree of redundancy. We are therefore considering all of the following possibilities:

1. The use of a solar diffuser whose degradation would be carefully monitored (1) by referring its solar-irradiated radiance to that of the sun, using a specially designed transfer spectroradiometer, and (2) by ratioing its solar-irradiated radiance to the radiance of the moon viewed directly by the instrument when within a $\pm 4^0$ phase angle.
2. The use of the moon as a radiance calibration source, again when within a $\pm 4^0$ phase angle. Our knowledge of the accurate absolute radiance of the moon under these conditions has been the subject of some debate and further study of this subject is underway.
3. The use of selected sites on earth for vicarious calibration purposes. This approach provides the best simulation of the operational image-acquisition geometry. There are basically two approaches to vicarious calibration: reflectance-based and radiance-based procedures, although a third using diffuse to global ratio irradiance measurements is also being pursued.
   * The reflectance-based procedure makes use of ground reflectance and optical depth measurements, made simultaneously with the image acquisition, and the use of the results in a radiative transfer code to predict the radiance at the instrument. This method has been shown to provide precisions of about ±3% for TM calibrations. Further improvements depend on the development of better ways to characterize the atmosphere, in particular the imaginary part of the aerosol refractive index. Of course these improvements are also vital for the improvement of the atmospheric correction procedures in general, research into which should be heavily emphasized between now and the start of the Earth Observing System missions in 1995.
   * The radiance-based method makes use of a calibrated spectroradiometer in a helicopter or high-altitude aircraft to sample the radiance of the area being imaged by a number of pixels in the satellite instrument. A relatively small atmospheric correction is required, since this method is usually conducted over White Sands, a high radiance scene.
4. Internal calibrator systems. The use of an internal calibrator is strongly recommended. This is based on (1) the stability of the TM internal calibrator, particularly for the first four TM bands, (2) its use in diagnosing the source of system degradation whether in the fore optics or in the filter/spectrometer-detector-electronics, and (3) for the redundancy it provides.

Cross-Calibration

Cross-calibrations can be affected by any of the above in-flight calibration procedures, except that using the internal calibrator. As an example, a potential use of a "robotic" arm would be to place the solar diffuser alternatively in front of MODIS and HIRIS and other similar instruments on the space platform.

In-Flight Response Characterization

Several instrument-response characteristics were discovered and studied as part of the LIDQA study on TM. The emphasis in future systems should be on the in-flight *validation* of the preflight characterization of the dynamic, micro-image response of the instruments rather than the discovery of these (to be hoped) small anomalies in flight. Some of these effects, such as those mentioned in above for TM amount to 2 to 3 digital counts which is significant if absolute uncertainty goals of $< \pm 3\%$ are to be implemented reliably under all conditions.

Spectral calibration has never been attempted on a multispectral remote-sensing satellite instrument but there is a critical science need for such a calibration. The spectrometer calibration is relatively easy. The calibration of filters can be achieved by the use of an auxillary spectrometer projecting spectra through the filters onto linear arrays.

This section is a paper, which we will submit to Remote Sensing of Environment in 1988.

III. SURFACE REFLECTANCE FACTOR RETRIEVAL FROM THEMATIC MAPPER DATA

Ronald G. Holm, M. Susan Moran,† Ray D. Jackson,†*
Philip N. Slater, Benfan Yuan, and Stuart F. Biggar

* Now at the Jet Propulsion Laboratory, Pasadena, California 91109.

† U.S. Department of Agriculture, Agricultural Research Service, US Water Conservation Laboratory, Phoenix, Arizona 85040.

The other authors are with the Optical Sciences Center, University of Arizona, Tucson, Arizona 85721.

Abstract

Based on the absolute radiometric calibration of the Thematic Mapper (TM) and the use of a radiative transfer program for atmospheric correction, ground reflectances were retrieved for several fields of crops and bare soil in TM bands 1 to 4 for six TM scenes acquired over a 16-month period. These reflectances were compared to those measured using ground-based and low-altitude, aircraft-mounted radiometers. When, for four TM acquisitions, the comparison was made between areas that had been carefully selected for their high uniformity, the results agreed to ±0.01 (1 σ RMS) over the reflectance range 0.02 to 0.55. When the comparison was made for two of the above acquisitions and two others on different dates, for larger areas not carefully selected to be of uniform reflectance, the results agreed to ±0.02 (1 σ RMS), again over the reflectance range 0.02 to 0.55.

Introduction

At the start of the Landsat program there was considerable interest in correcting Multispectral Scanner System (MSS) images for atmospheric effects in order to retrieve surface spectral reflectances. Examples are the papers presented at the Symposium on Significant Results of ERTS-1 in 1973 by Cousin et al., Fraser,

IV. AVHRR CALIBRATION

This work is being conducted to investigate improved vicarious methods for the calibration of MODIS-N and MODIS-T in-flight. It also provides calibration updates for FIFE and other purposes.

Method 1: Ground and Atmospheric Measurements and Reference to Another Calibrated Satellite Sensor

Ground reflectance measurements can be made over terrain areas corresponding to numerous Landsat TM pixels, but such measurements become impractical for the calibration of the AVHRR image data with pixel dimensions of 1.1 km by 1.1 km or greater. An alternative is to acquire AVHRR imagery of White Sands on the same day that a TM calibration has been carried out on the basis of ground reflectance factor and atmospheric measurements at Chuck Site in the alkali-flat region of White Sands. The methodology then takes advantage of the accurate calibration results for TM bands 3 and 4 to effect a calibration of AVHRR channels 1 and 2.

Figure IV.1 illustrates the steps in the calibration. A relatively uniform area corresponding to several AVHRR pixels is selected in the alkali-flat region and average digital counts are extracted for these AVHRR pixels and for pixels from the matching area in the TM imagery. With the help of radiative transfer computations and bidirectional reflectance data for the gypsum surface at White Sands, radiance at the entrance aperture of the AVHRR sensor is predicted. The analysis takes into account differences in spectral response, sun angle, and viewing geometry between the TM and AVHRR data acquisitions.

Method 2: Ground and Atmospheric Measurements with No Reference to Another Sensor

The second approach is analogous to the original reflectance-based approach used at White Sands to calibrate the TM or HRV sensors. Figure IV.2 shows the steps in this approach. It is based on detailed ground and atmospheric measurements at the time of AVHRR overpass, but it necessarily assumes the reflectance values to be representative of the whole pixel since these ground measurements can only encompass a portion of one AVHRR pixel. The availability of aircraft data can assist in the selection of an appropriately uniform area for this purpose. Although this method is not likely to be as accurate as the first, it has the distinct advantage of not requiring nearly coincident data acquisition from two different sensors.

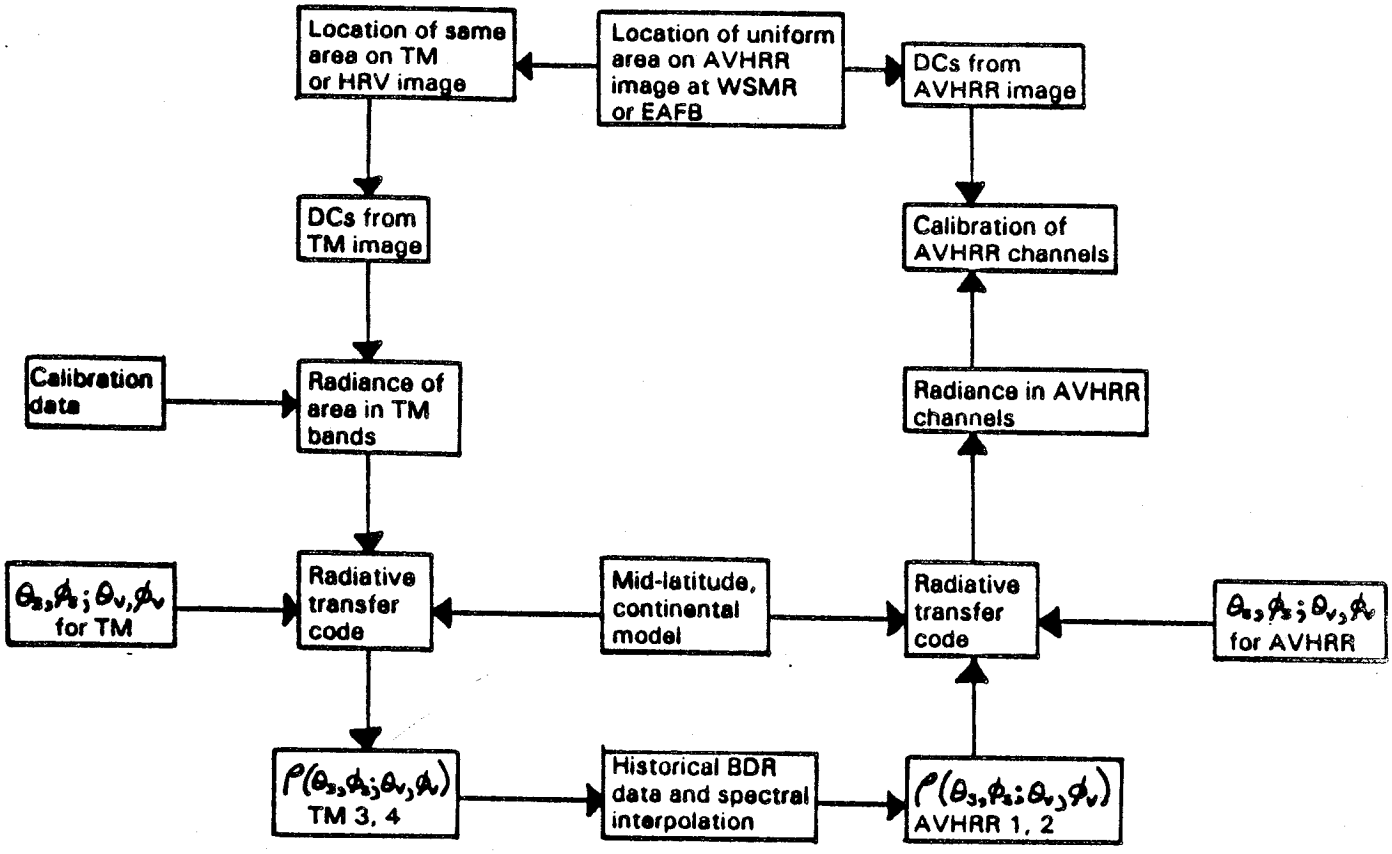

Figure IV.1. No ground and atmospheric measurements but reference to another satellite sensor.

Method 3: No Ground and Atmospheric Measurements but Reference to Another Satellite Sensor

This method is diagrammed in Figure IV.3. As with the first method, this approach achieves a calibration of the first two AVHRR channels by reference to another satellite sensor such as the TM on the same day. However, it differs significantly in that no ground and atmospheric measurements on the overpass day are needed. Instead, a standard data set of atmospheric conditions is used to approximate the actual atmosphere and historical bidirectional reflectance data are used to adjust for differences in illumination and viewing geometries. The same atmospheric parameters are adopted to estimate surface reflectance from the TM imagery and then to predict radiance at the AVHRR sensor from that surface reflectance (suitably adjusted for bidirectional effects and spectral bandpass

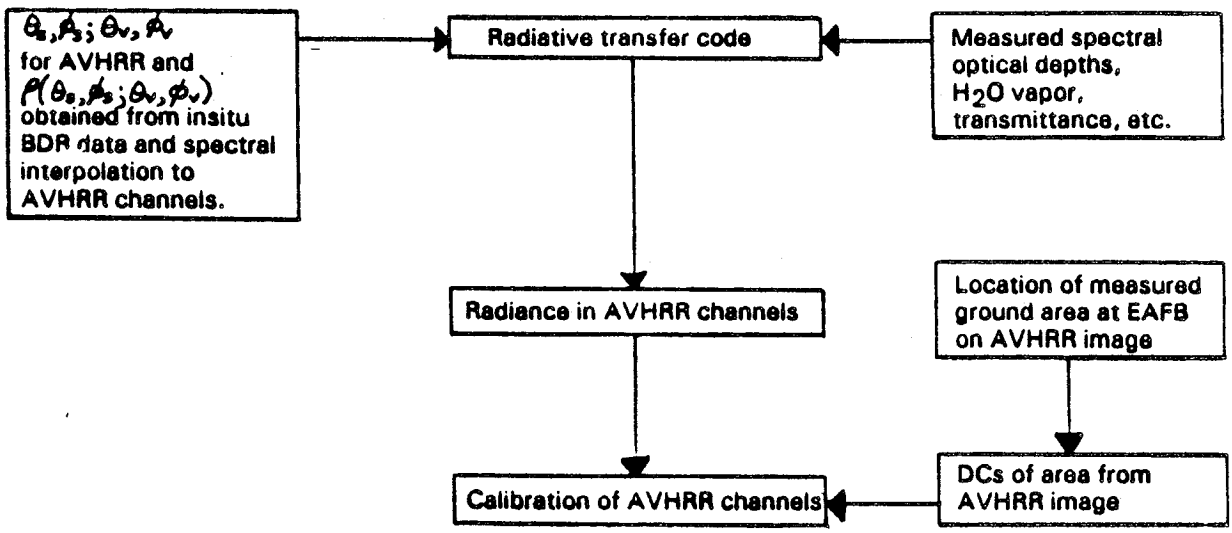

Figure IV.2. Ground and atmospheric measurements without reference to another sensor.

differences). Because of this two-way use of the atmospheric model, errors introduced in one direction will be compensated to some extent in the reverse direction so that reasonable calibration results can be obtained if the procedure is not overly sensitive to the choice of atmospheric model. If it proves to be viable, this approach will be a valuable one because it will facilitate in-orbit sensor calibration without the complexity and expense of field measurements.

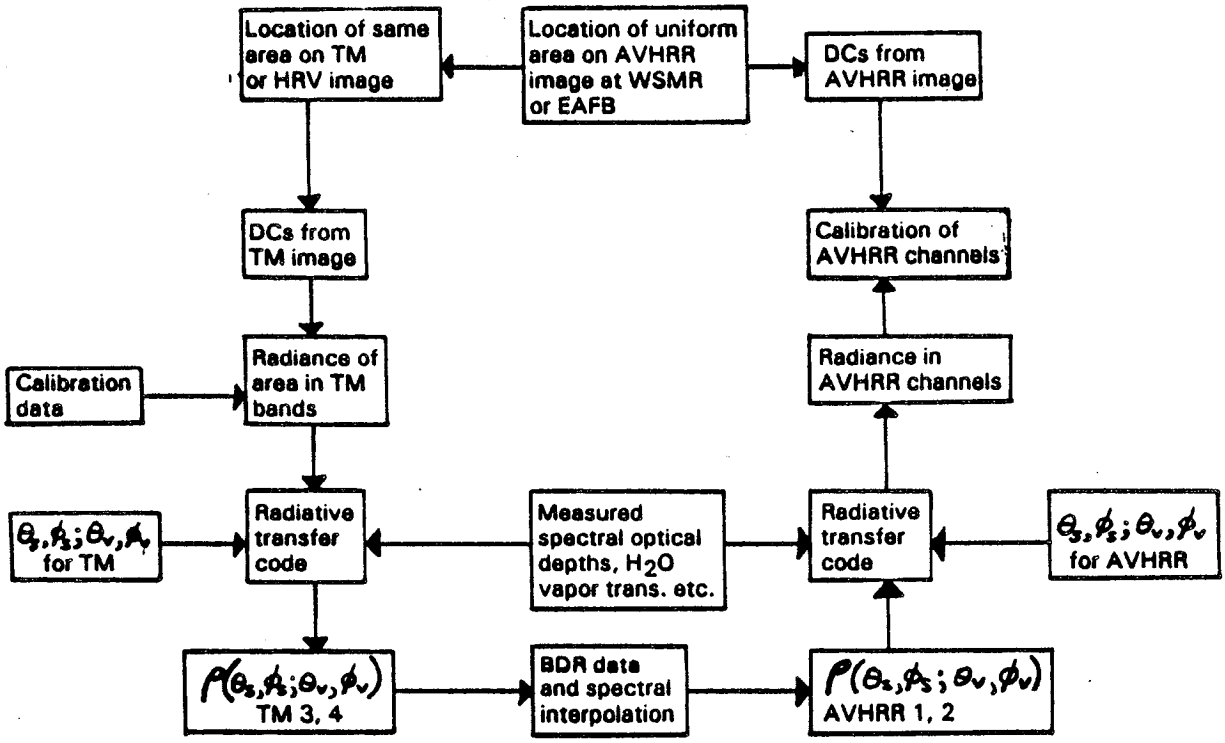

Figure IV.3. Ground and atmospheric measurements and reference to another calibrated satellite sensor.

V. THE IRRADIANCE-BASED METHOD

We start by reference to the basic remote sensing equation that relates the radiance at the sensor, or at the top of the atmosphere, L_S, to the radiance of the ground L_G, the transmittance of the atmospheric path between the ground and the sensor τ_A and the atmospheric path radiance L_P. The spectral dependence of these quantities will be omitted to simplify the notation thus:

$$L_S = L_G \tau_A + L_P. \tag{V.1}$$

We are interested in determining the ground reflectance ρ, where the surface is assumed horizontal, of infinite extent and lambertian and therefore the radiance of the surface is independent of azimuth. We designate the optical thickness δ, so Eq. V.1 can be rewritten

$$L_S = \frac{E_T \rho \exp(-\delta/\mu_v)}{\pi} + L_P . \tag{V.2}$$

where

E_T is the total (direct and diffuse) irradiance on the surface
$\mu_s = \cos \theta_s$, θ_s being the solar zenith angle and
$\mu_v = \cos \theta_v$, θ_v being the angle between the sensor's line-of sight and nadir.

We will follow the approach of Tanré et al. (1986) in decomposing E_T and L_P into their various components and deriving a relationship between the actual ground reflectance, ρ, and the apparent reflectance, or planetary albedo, ρ^*, as observed from space.

We can write

$$E_T = (E_{DIR} + \text{coupling term}) + (E_{DIF} + \text{coupling term}) \tag{V.3}$$

where the coupling terms account for multiple reflections between the earth's surface and the atmosphere respectively, the latter is described by S the spherical albedo of the atmosphere. This is illustrated in Figure V.1. Thus

$$E_{DIR} + \text{coupling term} = E_o \mu_s \exp(-\delta/\mu_s) (1 + \rho S + \rho^2 S^2 + \ldots) \tag{V.4}$$

or

$$E_{DIR} + \text{coupling term} = \frac{E_o \mu_s}{1 - \rho S} \exp(-\delta/\mu_s) \tag{V.5}$$

where E_o is the exoatmospheric solar irradiance.

We can write the diffuse irradiance incident on a surface of $\rho = 0$ as

$$E_{DIF} = E_o \mu_s \tau_d(\theta_s) \tag{V.6}$$

where $\tau_d(\theta_s)$ is defined as the downward-diffuse transmittance. With a non-zero value for ρ, we have the situation illustrated in Figure V.2. We can write:

$$E_{DIF} + \text{coupling term} = \frac{E_o \mu_s}{1 - \rho S} \tau_d(\theta_s). \tag{V.7}$$

Substituting Eqs. V.5 and V.7 into Eq. V.3 we get

$$E_T = \frac{E_o \mu_s}{1-\rho S} \{\exp(-\delta/\mu_s) + \tau_d(\theta_s)\} \tag{V.8}$$

for convenience we will write the total transmittance as:

$$\tau_T(\theta_s) = \frac{E_o \mu_s \{\exp(-\delta/\mu_s) + \tau_d(\theta_s)\}}{E_o \mu_s} \tag{V.9}$$

thus

$$E_T = \frac{E_o \mu_s \tau_T(\theta_s)}{1 - \rho S} . \tag{V.10}$$

Now the atmospheric path radiance term, L_P, can be decomposed into L_{IP}, the intrinsic path radiance, that is the path radiance when $\rho = 0$, and a term L_{EA} due to the earth-atmosphere coupled irradiance reflected from outside the sensor's IFOV that only enters the IFOV because of atmospheric scattering as shown in Figure V.3. Thus Eq. V.2 can be rewritten

$$L_S = \frac{E_T \rho \exp(-\delta/\mu_v)}{\pi} + L_{IP} + L_{EA}. \tag{V.11}$$

L_{EA} is a product of the surface reflectance ρ, the total surface irradiance, and the upward diffuse transmittance, $\tau_d'(\theta_v)$

$$L_{EA} = \frac{E_T \rho \, \tau_d'(\theta_v)}{\pi} . \tag{V.12}$$

By Helmoltz's theorem of reciprocity the functions $\tau_d'(\theta_v)$ and $\tau_d(\theta_v)$ are identical. Substituting Eq. V.11 into V.10 we have

$$L_S = \frac{E_T \rho}{\pi} \{\exp(-\delta/\mu_v) + \tau_d(\theta_v)\} + L_{IP} . \tag{V.13}$$

By writing the total transmittance along the sensor's line-of-sight as $\tau_T(\theta_v)$ and substituting Eq. V.10 in Eq. V.13 we have

$$L_S = \frac{E_o \mu_s \rho \tau_T(\theta_s) \tau_T(\theta_v)}{\pi (1 - \rho S)} + L_{IP}. \tag{V.14}$$

This is the basic equation for determining the total radiance at the entrance pupil of the space sensor due to the earth-atmosphere system. We can write L_S in terms of an apparent reflectance ρ^*,

$$L_S = \frac{\rho^* E_o \mu_s}{\pi} \tag{V.15}$$

and the intrinsic path radiance in terms of an effective atmospheric reflectance ρ_A,

$$L_{IP} = \frac{\rho_A E_o \mu_s}{\pi} . \tag{V.16}$$

Substituting Eq. V.15 and V.16 in Eq. V.14 we have

$$\rho^* = \frac{\rho \tau_T(\theta_s) \tau_T(\theta_v)}{1 - \rho S} + \rho_A . \tag{V.17}$$

Inserting the angular and spectral dependencies that, for convenience, have been omitted thus far, we have the basic equation

$$\rho^*(\theta_s; \theta_v, \phi_v; \lambda) = \frac{\rho(\lambda) \tau_T(\theta_s; \lambda) \tau_T(\theta_v; \lambda)}{1 - \rho(\lambda) S(\lambda)} + \rho_A(\theta_s; \theta_v, \phi_v; \lambda) . \tag{V.18}$$

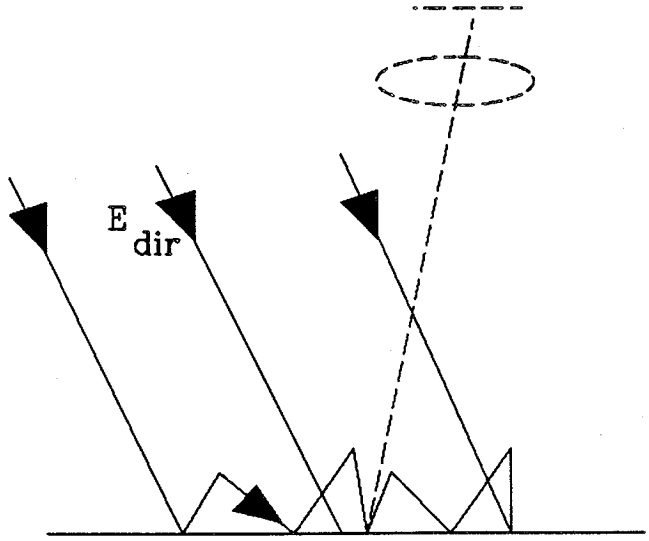

Figure V.1. Direct irradiance of imaged area and diffuse coupling term.

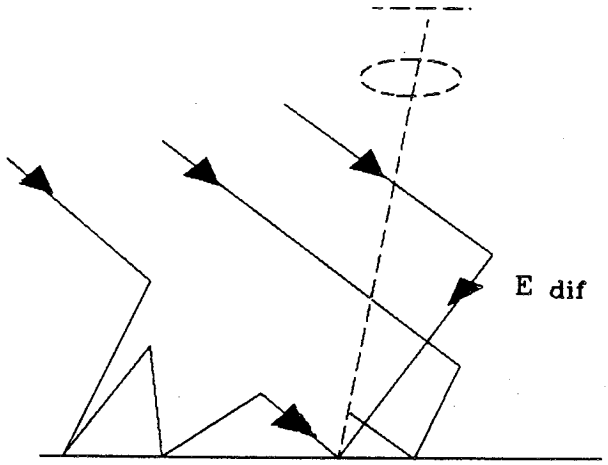

Figure V.2. Diffuse irradiance of imaged area and diffuse coupling term.

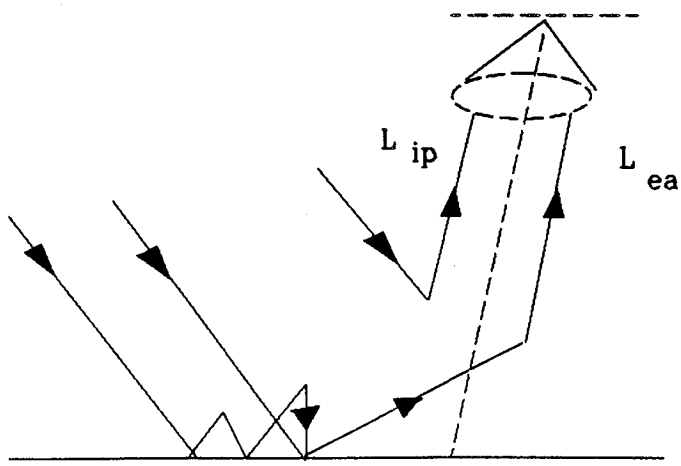

Figure V.3. Intrinsic path radiance and path radiance due to earth-atmosphere coupled irradiance reflected from outside the sensor's FOV but scattered into it.

Tanré et al. have derived approximate expressions that account for a difference in reflectance between the small area being imaged and its surround.

In the first case, the surrounding is assumed uniform, lambertian and of reflectance ρ_{us}. The reflectance, ρ, used in the coupling term $1-\rho S$ in Eq. V.10 and the reflectance term used in Eq. V.12 have to be replaced by ρ_{us}. Thus Eq. V.13 becomes

$$\rho^* = \frac{\tau_T(\theta_s)}{1 - \rho_{us}S} \{\rho \exp(-\delta/\mu_v) + \rho_{us}\tau_d(\theta_v)\} + \rho_A. \qquad (V.19)$$

In the second case, for which the surround is of non-uniform reflectance, ρ_{us} in Eq. V.19 should be replaced by ρ_{ns} which represents a spatial average of reflectances across the surround, weighted by an atmospheric function to account for proximity to the area being imaged. Tanré et al. define ρ_{ns} as

$$\rho_{ns} = \frac{1}{\tau_d(\theta_v)} \iint_{-\infty}^{\infty} \rho'(x, y)\, e(x, y, \theta_v)\, dx\, dy \qquad (V.20)$$

where $\rho'(x, y)$ is the diffuse reflectance of a point, M, in the surround, distance x, y from the area being imaged. $e(x, y, \theta_v)$ is the contribution of the downward diffuse transmittance $\tau_d(\theta_v)$ per unit area due to the α surface at M.

This is not an exact formulation. However, because the influence of the adjacency effect is often difficult to detect in remote sensing imagery, the correction accuracy need not be high.

Tanré et al. suggest an approximate correction for absorption by multiplying the terms on the right hand side of Eqs. V.18 or V.19 by

$$\tau_g(\theta_s, \theta_v) = \prod_{(i=1)}^{4} \tau_i(\theta_s, \theta_v, u_i) \qquad (V.21)$$

where:

$\tau_g(\theta_s, \theta_v)$ is the total gaseous absorption along downward and upward paths through the atmosphere;

i designates the absorber: ozone, water vapor, carbon dioxide, or oxygen;

u is the concentration of the absorber.

Equations 17, 18, or 19, together with Eq. 21, can be used to determine the apparent reflectance from a knowledge of the ratio α, of the diffuse irradiance incident on an area in the shadow of a small opaque parasol, E_P, to the total or global irradiance, E_T, at the ground. Note we distinguish E_P from E_{DIF} in Eq. V.7 because the latter assumes no contribution from coupled direct irradiance at the ground i.e. either $\rho = 0$ or that the shadow exists over an extensive area such that the coupling term can be neglected. E_P in contrast, is the sum of the coupled ground irradiance from outside the shadowed area and E_{DIF} from Eq. V.7, thus

$$E_P = E_o\mu_s \exp(-\delta/\mu_s) \{\rho S + \rho^2 S^2 + \ldots\} + \frac{E_o\mu_s\tau_d(\theta_s)}{1 - \rho S} \tag{V.22}$$

$$= \frac{E_o\mu_s}{1 - \rho S}\{\rho S \exp(-\delta/\mu_s) + \tau_d(\theta_s)\} \tag{V.23}$$

therefore, from Eq. V.8 for E_T and Eq. V.23 for E_P,

$$\alpha_s = \frac{E_P}{E_T} = \frac{\rho S \exp(-\delta/\mu_s) + \tau_d(\theta_s)}{\exp(-\delta/\mu_s) + \tau_d(\theta_s)} \tag{V.24}$$

But from Eq. V.9,

$$\tau_T(\theta_s) = \exp(-\delta/\mu_s) + \tau_d(\theta_s) \ . \tag{V.25}$$

Eliminating $\tau_d(\theta_s)$ from Eqs. V.24 and V.25 we have

$$\tau_T(\theta_s) = \frac{(1 - \rho S)\exp(-\delta/\mu_s)}{1 - \alpha_s} \tag{V.26}$$

and from Helmholtz's reciprocity theorem we know that the transmittance along the angle of view to nadir, θ_v, is given by

$$\tau_T(\theta_v) = \frac{(1 - \rho S)\exp(-\delta/\mu_v)}{1 - \alpha_v}. \tag{V.27}$$

Substituting Eqs. V.26 and V.27 into Eq. V.17 and accounting for gaseous transmittance, τ_g, as described by Eq. V.21, we have

$$\rho^* = \tau_g \left\{\frac{\rho(1 - \rho S)\exp(-\delta/\mu_s)\exp(-\delta/\mu_v)}{(1 - \alpha_s)(1 - \alpha_v)} + \rho_A\right\} \tag{V.28}$$

α_s, δ, and ρ can be measured at the time the satellite sensor acquires the image of the measured area, μ_v and μ_s are determined from a knowledge of the time of acquisition. α_v is found by extrapolating the α values, collected during the morning, to the solar angle equal to the nadir view angle of the satellite. τ_g is decomposed into its various components. τ_{ozone} is found from Langley plot data or from results from the Total Ozone Mapping System. τ_{H_2O} is found from relative humidity and temperature measurements taken at ground level or from radiosonde or solar radiometer data. τ_{CO_2} and τ_{O_2} are taken from published data. Using these values as input to the 5-S code, values for S and ρ_A can be found. All the quantities are then available for the calculation of ρ^* in Eq. V.28.

Reference

Tanré, D. Deroo, C., Dahaut, P., Herman, M., Morcrette, J. J., Perbos, J., and Deschamps, P. Y. (1985) Effets atmospheriques en teledetection - logiciel de simulation du signal satellitaire dans le spectre solaire, Proceedings of the 3rd International Colloquium on Spectral Signatures of Objects in Remote Sensing, ESA SP-247 pp. 317-319.